Chapter

High-Resolution Ultrasound Imaging System for the Evaluation of the Vascular Response to Stent or Balloon Injuries in the Rabbit Iliac Arteries

Aurélien Frobert, Guillaume Ajalbert, Jérémy Valentin, Stéphane Cook and Marie-Noëlle Giraud

Abstract

For novel therapeutic approaches of cardiovascular diseases, the preclinical investigation is of paramount and required appropriate technologies. We investigated the use of high-resolution ultrasound imaging system to evaluate the progression of vascular lesions in a rabbit model. Animals underwent vascular injury using two standard procedures. A bare-metal stent was placed within the left iliac artery, and a balloon injury was induced in the contralateral artery. The animals were kept on a regular diet for 8 weeks. A Vevo3100© VisualSonic high-resolution ultrasound imaging system and the associated software VevoVasc were used for the longitudinal evaluation of the injured arteries and the distal abdominal aorta. The lumen size increased rapidly after the intervention in both iliac arteries. In the balloon-injured artery, the augmentation was transient and significantly reversed, inducing an alteration of the blow flow. In contrast, in the stented segment, the lumen size was maintained enlarged overtime. We demonstrated a significant correlation for the wall thickness and the lumen size between ultrasonic and histological quantification. High-resolution ultrasound imaging in rabbit iliac arteries and the distal abdominal aorta is feasible, reliable and of relevance to investigate novel strategies for the inhibition of hyperplasia induced with standard injury models.

Keywords: echography, iliac arteries, vascular stent, rabbit, longitudinal study

1. Introduction

Coronary heart diseases remain a prominent cause of morbidity and mortality [1]. Percutaneous coronary intervention (PCI) is the current standard treatment and aims to widen the lumen, restore the blood flow into the vessel and consequently re-perfuse the ischaemic myocardium. A catheter is fed through the femoral artery until the blocked coronary and the balloon inflated. A stent is then placed and maintains the artery opened to limit adverse vessel remodelling and elastic recoil.

Since 2003, the standard of care is the balloon-expandable, drug-eluting metallic stent. Steady improvement of stent technology promoted a rapid evolution from the

first generation of the bare-metal stents (BMS, permanent metallic structure without drug release) to the last generation of drug-eluting stents (DES, permanent metallic structure with anti-proliferative drug release). The BMS and DES are mostly made of a cobalt-chromium alloy and remain lifelong in the artery of the patient. Several studies showed, however, that life-threatening complication, emerging several months or years after implantation, may occur, including restenosis due to neointimal hyperplasia and late in-stent thrombosis [2]. Novel therapeutic approaches to reduce persistent inflammation, stenosis and thrombosis are focused on anti-proliferative and anti-inflammatory processes such as drug-eluting stents [3], pharmaceutical [4, 5] or laser-based approaches [6, 7] as well as bioresorbable stents [8].

In this context, an appropriate animal model is paramount to foster the development of new therapies, to provide in vivo preclinical proof of concept, to evaluate the treatment performance and to promote translation to the clinic. The rabbit-injured iliac artery model has been well established to investigate the vascular response to hyperplasia and stenosis or thrombosis [3, 8, 9].

In the present study, we evaluated the vascular responses to bilateral iliac artery injuries performed by balloon denudation and stent overexpansion, using a high-resolution ultrasound imaging system. We explored the longitudinal evolution of the vessel morphometries and the blow flow.

2. Methods

Three male New Zealand white rabbits (3.5–4 kg) were obtained from the Charles River Laboratories, France. The animals were housed in the animal centre facility at the University of Fribourg (Switzerland). All animals received humane care in compliance with the European Convention on Animal Care and in accordance with the Swiss Animal Protection Law after obtaining permission from the State Veterinary Office, Fribourg approved by the Swiss Federal Veterinary Office, Switzerland (FR-2016/16).

Angioplasty: Under general anaesthesia induced with s.c. injection of Narketan (65 mg/ml) and Xylapan (4 mg/ml) and maintained by perfusion (Narketan 65 mg/50 ml, Xylapan 4 mg/50 ml, infusion 15–20 ml/h), heparin (100 UI/ml) was administered in the marginal vein using a 24 GA (BD Insyte) catheter. Body parameters, including temperature, heart rate and pO_2 were controlled by a veterinary monitor (Midmark Cardell touch). In clean condition, an arteriotomy of the left coronary artery was performed, and a 6-French introducer sheath (Glidesheath Slender, Terumo) positioned. Two ml of a contrast agent (Bracco, Iomeprol 35 g) was injected, and a 0.36-mm guidewire is advanced through an introducer sheath up to the right iliac artery. Under angiographic monitoring of the pelvic area (**Figure 1**), the stent from Baxter (Coroflex Blue Neo) was deployed and overexpanded. The balloon was then retracted and then directed within the contralateral iliac artery (left), positioned at the same distance from the aortic bifurcation and inflated at 10 atm for 30 seconds to induce endothelial injury. At the end of the procedure, s.c. injection of Temgésic (1 ml/kg), Trimethazol (Werner Stricer, composed of sulfadoxine 40 mg/kg and trimethoprim 8 mg/kg) and carprofen 2.2 mg/kg (Rimadyl, Zoetis) were performed. The rabbit awoke within 1 h. Animals were kept on a normal diet for up to 8 weeks.

High-resolution ultrasound image acquisitions were performed every week under general gaze anaesthesia induced by isoflurane 4–5% and O_2 2–3 L/h. The animals were placed on an in-house-made platform, on a heating pad. The animal temperature was monitored through the rectal probe provided with the Vevo3100. ECG stainless steel needle electrodes provided with the Vevo3100 were placed

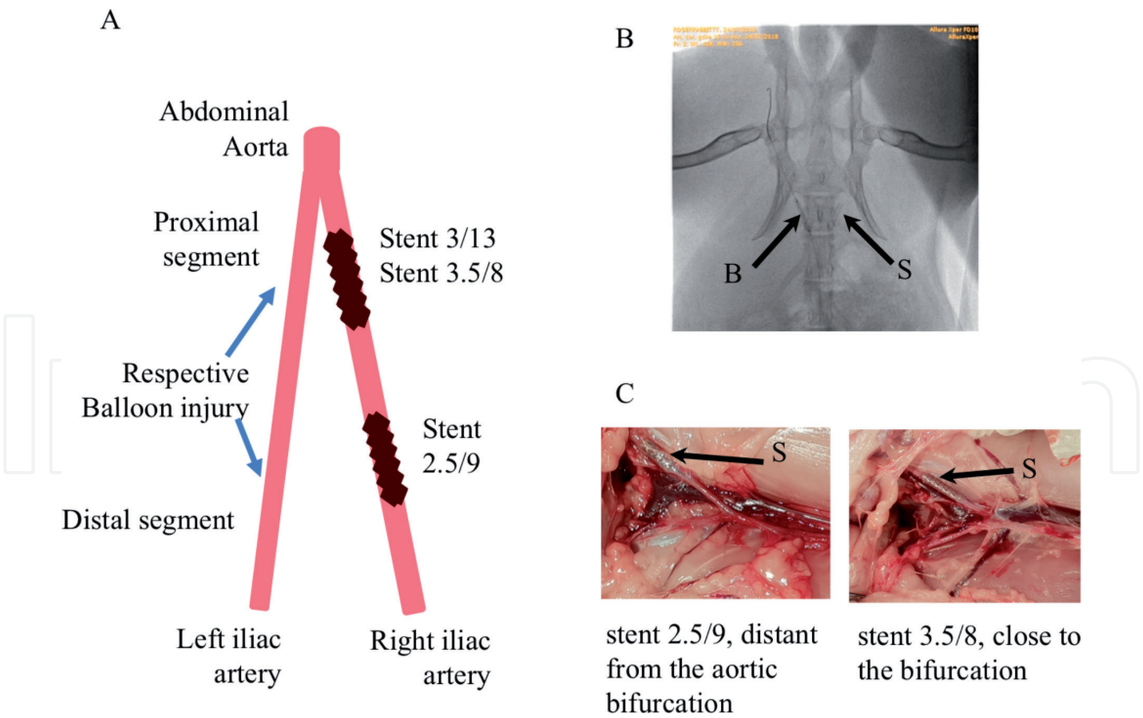

Figure 1.
Bilateral iliac artery injuries performed by an inflated balloon (left artery) and stent overexpansion (right artery). (A) Diagram showing the positioning of the stent and contralateral balloon placement. Each animal received a single stent that was placed either close to the aortic bifurcation or distally. (B) Angiography of both iliac arteries: The stent was placed first in the right artery and overexpanded, and the balloon was then retracted back to the aorta and introduced into the left artery. Balloon inflation was performed at a similar distance from the aortic bifurcation. S, stent; B, balloon. (C) Illustration of the positioning of the stent: 8 weeks post-intervention, the right iliac was exposed, and the transmural visualisation of the stent confirmed the site of the stent placement.

subcutaneously on the four limbs (right and left upper, right and left lower). The respiration rate was derived from the ECG signal. Longitudinal analyses were performed with a Vevo3100, VisualSonic high-resolution ultrasound system equipped with a transducer MX400 (20–46 Mhz) hold with the imaging station arm. The images were acquired at day 0, 14, 28, 42 and 56 or 63 in all animals. The image analyses were performed with the VevoVasc analysis module. The following parameters were quantified: wall thickness, lumen diameter and cross-sectional area (CSA). Using a Doppler pulse-wave mode, the velocity-time integral (VTI) was extracted. The following calculation was performed with the measured parameters: the blood flow was calculated as the product of the VTI and the CSA of the respective segments. The percentage changes in parameters relative to the values before the intervention were calculated as a ratio of the parameter at day 14, 28 or 42 to the same parameter at day 0 and multiplied by 100.

Artery harvesting was performed after euthanasia. Distal aortic segment and both iliac arteries were harvested according to the well-established procedure [10] and cut in short segments for histological analysis.

Histology characterisation: OCT embedding the vessel segments was frozen in the vapour of 2-methylbutane placed in liquid nitrogen. Sections of 5 μm are obtained using a cryocut and were processed for Movat Pentachrome staining. Briefly, sections were fixed 1 h in Bouin for 56°C, stained with Alcian Blue followed by Verhoeff's Elastic Stain, differentiated in ferric chloride solution, stained in brilliant crocein 1% and acid fuchsin 1%, placed in 5% phosphotungstic acid and stained with crocin. Sections were mounted with EUKITT®.

Stented segments were embedded in epoxy. 0.8-μm sections were cut with an ultramicrotome and stained with methyl blue.

The Bersoft Image Analysis software (Bersoft Technology and Software; Lunenburg, Canada) was used to quantify the vessel diameter and the wall thickness (including intimal, media and adventitia layers).

2.1 Statistics

Values are presented as mean ± SEM. The percentage changes in wall thickness, cross-sectional area and blood flow were analysed using two-way ANOVA; Fisher's LSD multi-comparisons were performed for the different segments and for the time effect. Linear regression and the parametric Pearson test were computed in a two-tailed manner. Analyses were performed using Prism software. Values were considered significantly different when $p < 0.05$.

3. Results

3.1 Stent placement

We report the results from three rabbits that received a Coroflex Blue Neo BMS. In concordance with the standard clinical procedure, each animal received a stent with an appropriate diameter defined under angiographic monitoring. The respective diameter (mm) and length (mm) of the stents were 2.5/9, 3/13 and 3.5/8. The stent positioning and contralateral balloon injury were proximal from the abdominal aortic bifurcation for the two animals and distal for one animal, as shown in **Figure 1**. The interventions were performed successfully without complication. All animals appeared healthy without significant weight loss. No infection, oedema or arterial thrombosis was encountered. The wound area was normal.

3.2 Morphometry: longitudinal quantification

The ultrasonographic vascular parameters were recorded before and after stenting or balloon injury every second week up to 8 weeks to evaluate the vessel structure. The imaging and measurements were performed at the injured and stented segments of the arteries as well as at the intact segments free from intervention situated distally and proximally of the lesion or stent, as controls (**Figure 2A**). The distal part of the abdominal aorta was also imaged and analysed (**Figure 2B**).

We report in **Figure 2A** the values of the diameters and wall thicknesses of the stented and balloon-injured iliac arteries obtained for each animal. We chose to present each animal data to visualise the individual variations. For instance, after balloon injury, the vessel diameter increased transiently up to 14 days at the site of the injury. However, for two animals the diameter returned to initial size while staying enlarged for the third animal. A transient vessel enlargement was also observed for the distal and proximal controls. Likewise, the aorta wall thickness followed three different evolutions from day 14 to day 60 when considering each animal separately, the aorta wall thickness increased consistently for one animal (that received 3.5/8 the stent), alternate phases of augmentation and diminution for the second one (stent 3/13), while it decreased for the last rabbit (stent 2.5/9) after a transient increase (**Figure 2B**).

For the iliac arteries, as presented in **Figure 2C**, we calculated the mean percentage changes both, the wall thickness and the CSA relative to the pre-intervention. We showed a change of the wall thickness at the site of the stent. At day 14, the wall

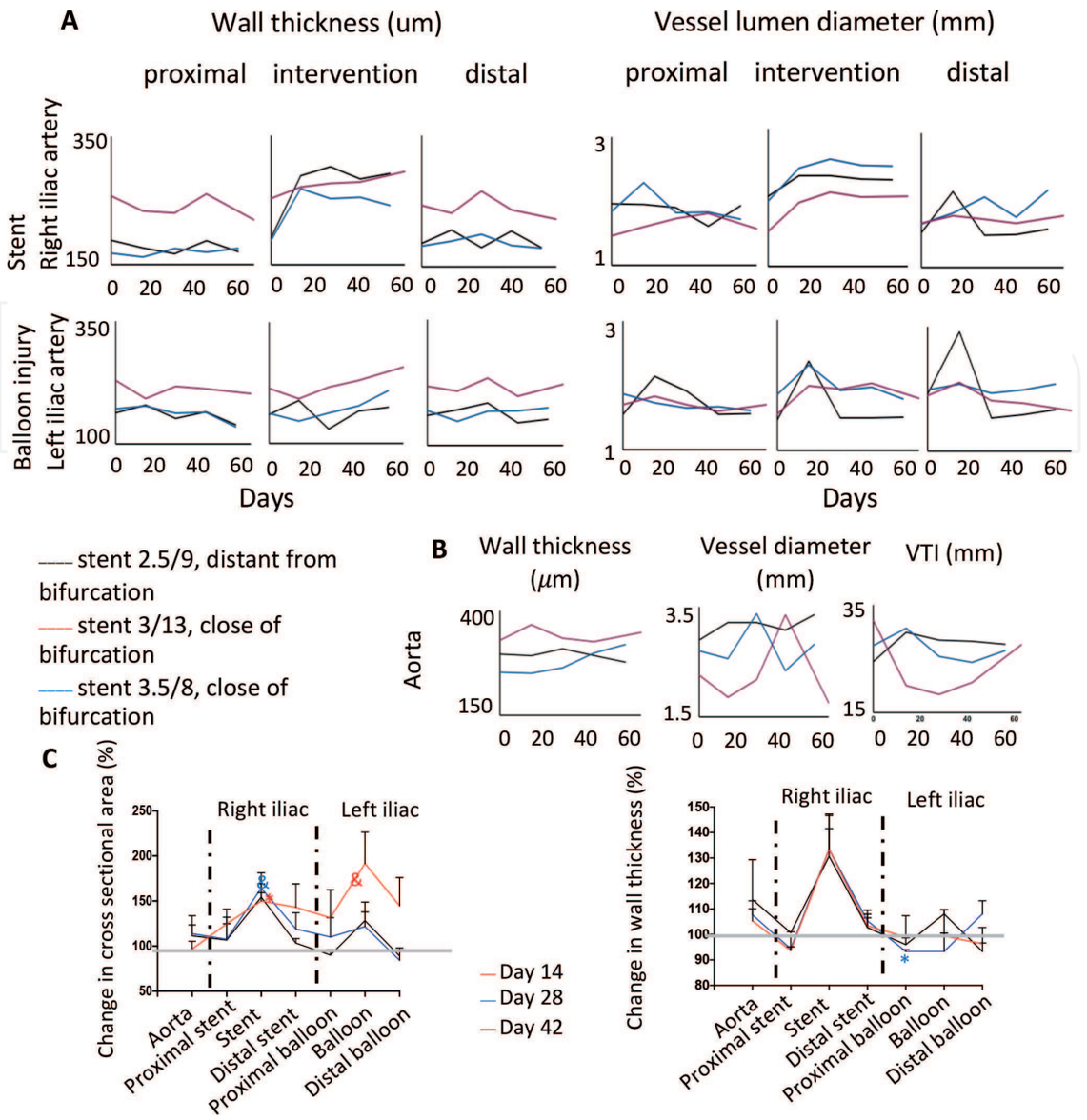

Figure 2.
*Longitudinal evaluation of the vessel structure. (A) The longitudinal measurements of the wall thickness and the lumen diameter of the right and left iliac arteries performed in different segments: at the site of the intervention (i.e. stent placement for the right artery and balloon inflation for the left artery) and at the proximal and distal uninjured segments as controls. Each animal and the corresponding stent are indicated and represented by a colour line. (B) Structure and VTI measured at the distal abdominal aorta. (C) Percentages of change in the crosssectional area of the vessel and the wall thickness relative to day 0 (preintervention, grey line) represented according to the vessel segment. Each line represents a different time post-intervention (day 14, 28 and 42). The results are shown as the mean of three animals and SEM. * $p < 0.05$ vs. day 0 and $p < 0.05$ vs. distal and proximal control segments.*

thickness showed a 133 ± 13% increase as compared with pre-intervention. For the proximal control segments, the wall thickness was not significantly altered over time.

In contrast, following balloon injury, the wall thickness remained constant, over time with a slight, but statistically significant, reduction (94 ± 1%, $p = 0.01$) observed after 42 days in the proximal segment.

In parallel, we report a significant increase (150 ± 9%, $p = 0.03$) in the CSA in the stented segment. The CSA remained elevated over time.

In contrast, the lumen CSA transiently increased in the left artery. The maximal significant change was 192 ± 35% in the injured segment as compared to the proximal (131 ± 31%, $p = 0.02$) and distal (145 ± 31%, $p = 0.006$) controls at day 14. The lumen area returned then to initial values.

3.3 Blood flow

Employing a pulsed wave (PW) Doppler mode, we recorded the velocity, extracted the velocity-time integral (VTI) and calculated the blood flow. As presented in **Figure 3**, for each animal, VTI gradually decreased over time in both, the balloon and stent-injured areas, and consequently in the distal control except for one animal.

Overall, in the right artery, there was no significant difference in the mean percentage changes of the blood flow in the stented segments (**Figure 3C**) although a maximal mean reduction of 72 ± 12% was observed at day 14. Looking at the individual data of the VTI, we observed a large variability. In contrast, in the left artery, the longitudinal analysis showed a significant change of the

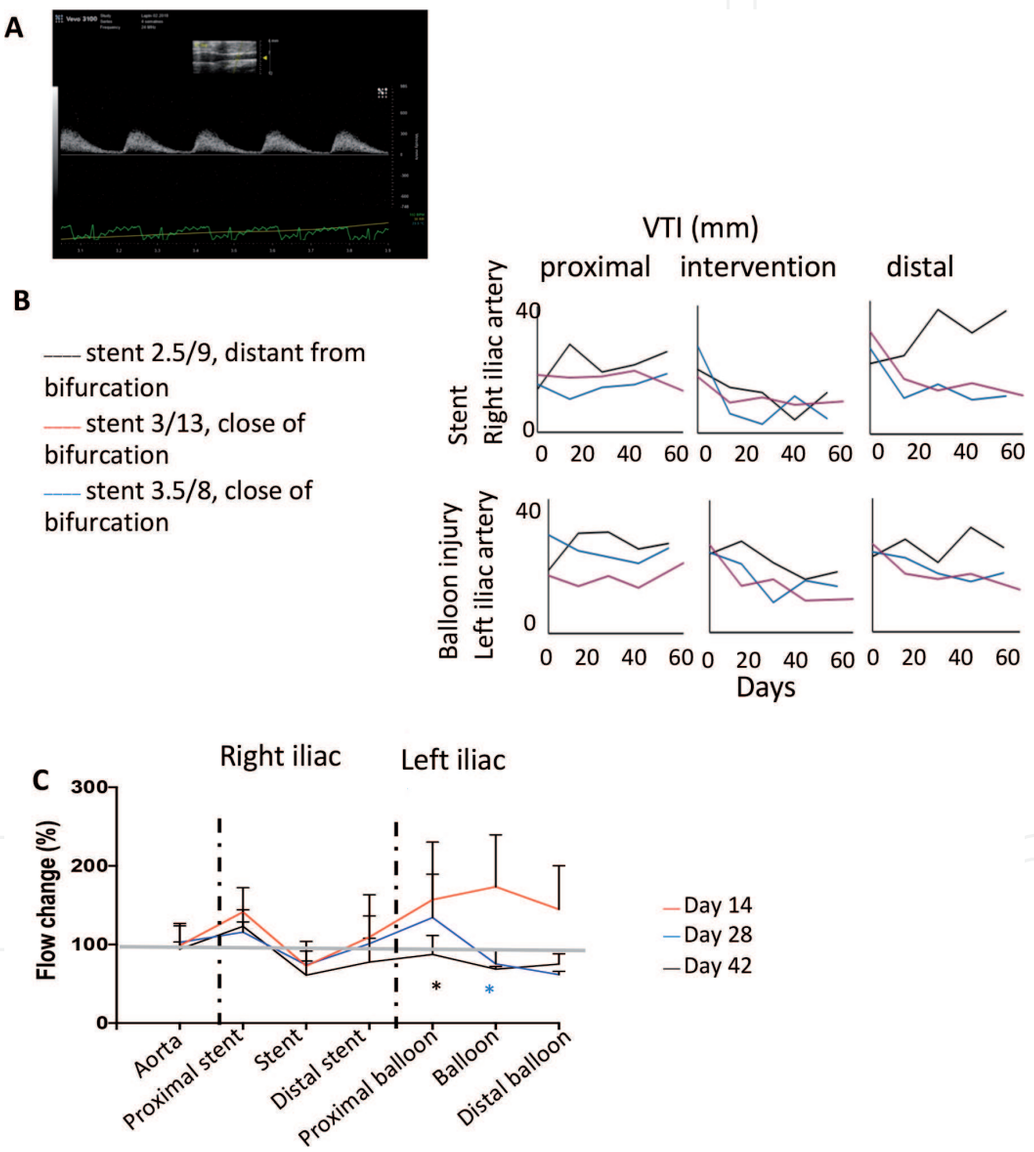

Figure 3.
*Height and weeks for longitudinal evaluation of the VTI and blood flow. (A) Illustration of the PW Doppler recording of left stented iliac artery velocity. The measurements were performed in the distal segment. (B) The measurements of the VTI in the right and left iliac arteries before (day 0) and post-intervention were performed in different segments: at the site of the intervention—Stent placement for the right artery and balloon inflation for the left artery and at the proximal and distal uninjured segments as controls. Each animal and the corresponding stents implanted are indicated and represented by a colour line. (C) Percentages of change in the blood flow relative to day 0 (pre-intervention, grey line) represented in the function of the vessel segment. Each line represents a different time post-intervention (day 14, 28 and 42). The results are shown as the mean of three animals and SEM * $p < 0.05$ vs. day 0.*

blood flow, respectively, 62 ± 4% (p = 0.01) at day 28 in the distal segment, and 68 ± 3% (p = 0.01) recorded at day 42 in the left iliac artery. The transient increase of the blood flow observed at day 14 (173 ± 66%) was not statistically significant.

3.4 Endpoint measurement: comparison between ultrasound measurement and histology

The lumen diameters at seven sites of the iliac arteries and aorta in the three rabbits subjected to balloon injury and stenting were quantified using both high-resolution ultrasound and histology. The correlations between the measurements performed by ultrasound and the histological analysis of the vessel diameter and the wall thickness, 8 weeks after the intervention, are presented in **Figure 4A**. We demonstrated a significant correlation between the two analytical procedures for both parameters, respectively, for the vessel diameter, $r^2 = 0.5$, p = 0.006 and for the wall thickness, $r^2 = 0.21$, p = 0.04. The thickening of the intima was observed prominently in the stented segment (**Figure 4B**) and for one animal in the distal area of the balloon-injured segment (**Figure 4C**). Alignments were performed on the different parts of the figures.

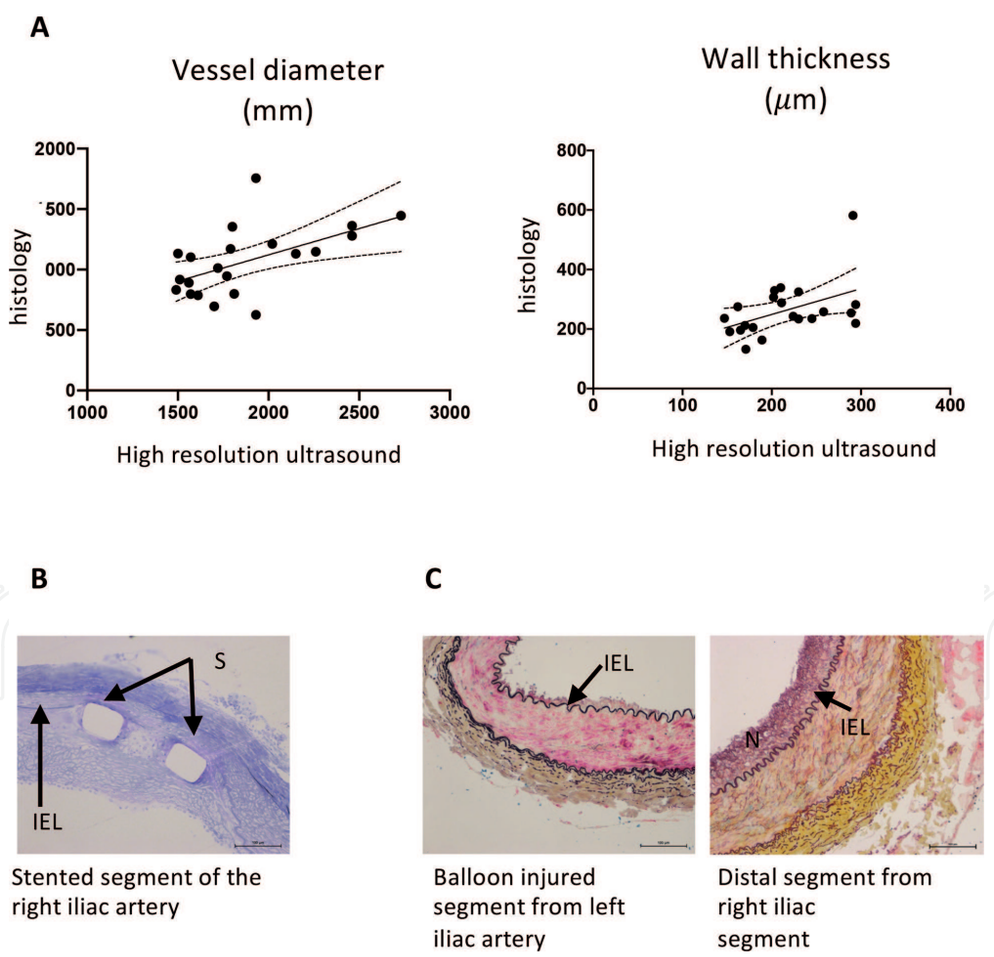

Figure 4.
Histology evaluation of rabbit iliac arteries. (A) Correlation between the high-resolution ultrasound and histological measurements of the vessel diameters and wall thicknesses. The individual dots represent each value obtained in all the segments assessed 8 weeks post-intervention. (B) Representative methyl blue stained histologic cross section of an 8-week rabbit-stented right iliac artery showing the intimal hyperplasia. The staining pattern shows prominent intimal thickening in the stented segment of the iliac artery. S indicates the stent struts. (C) Movat Pentachrome stained histologic cross section of a rabbit left iliac artery 8 weeks after the balloon injury. N indicates luminal neointimal formation. Arrow indicates internal elastic lamina (IEL).

4. Discussion

Mechanical endothelium injury is a standard strategy to induce hyperplasia in various animal models such as mice, rabbits or minipigs [9, 10, 17]. In the present study, the endothelial injury was induced by two different approaches in rabbits: first by overexpansion of a BMS in the right iliac artery and second with an inflated balloon in the contralateral left iliac artery. Stenting and balloon injury resulted in a respective permanent and transient overexpansion of the vessel inducing a well-recognised vascular response [11]. An acute inflammation rapidly follows the induced endothelium injury or denudation and peaks after a few days; then, the inflammation temporally declines during the resolution phase. Acute inflammation is accompanied by the proliferation of smooth muscle cells that results in hyperplasia. Consequent thickening of the wall (hyperplasia) may induce a narrowing of the vessel lumen (stenosis) and reduction of the blood flow.

In the present study, we showed that the rabbit iliac arteries and the distal abdominal aorta could be successfully monitored using high-resolution ultrasound for longitudinal and non-invasive investigation. The quality of the images acquired allowed rigorous measurements of the wall and vessel sizes. It is important to note that for some measurements, the possible presence of oedema could impair the quality of the image acquisition and may explain variations of the parameters in consecutive weekly measurements.

Besides, the metallic structures of the BMS were visualised as shadows. Although the presence of the metallic stent did not impair the wall thickness and vessel diameters' quantification, the blood flow velocity measurements were often challenging to perform.

Comparing the acute balloon injury with the chronic injury associated with stent implantation, we reported that the response of the vessel differed with the type of intervention. The primary function of the BMS stent is to provide mechanical support. As expected, the stent allowed the maintenance of increased vessel diameter in all animals. In contrast, balloon inflation induced a short-term increase in the lumen size followed by a reduction suggesting a weakening of the artery.

Notably, the overexpansion of the stent affected the wall thickness that increased rapidly and remained elevated. Histology analysis revealed the formation of neointimal hyperplasia. In contrast, balloon injury results in a transient wall thickening recorded 2 weeks post-intervention with a successive return to the initial dimensions. Transient inflammatory response to the balloon injury may explain the wall. Accordingly, Welt et al. [12] reported a transient inflammation following a balloon injury model as compared with a sustained accumulation of inflammatory cells such as monocytes in stented iliac arteries of rabbits up to 14 days.

Furthermore, Virmani et al. [13] reviewed the temporal vascular response to BMS implanted in the rabbit iliac artery. Between 7 and 14 days, the intimal thickness increased due to inflammation and cell proliferation and then peaked at 1 month with a return of the cell proliferation to the basal level. Further shrinkage has been reported from 3 to 6 months due to the extracellular matrix remodelling. In agreement, we also report the shrinkage of the wall thickness observed at day 28 in the left artery.

As far as the evaluation of the blood flow is concerned, the VTI and the calculated changes in flow revealed notable individual variations. Nevertheless, the longitudinal evaluation showed that in all animals, the VTI decreased overtime in the left and right segments but remained stable in the proximal segments. Meanwhile, the calculated blood flow was significantly reduced at the site of the balloon injury and the distal segment but maintained unchanged in the stented segment.

Despite the neointimal hyperplasia developed within the stent, the blood flow was maintained due to the diameter enlargement resulting from the stent overexpansion. Nevertheless, it is essential to note a maximal 72% reduction of the blow flow, although the statistical significance was not reached due to the small number of animal and large variability.

The aorta underwent twice the passage of the catheter, once with the crimped stent followed by its retraction and second with the successive introduction into the contralateral artery. The vessel structure remained similar in all the animals, suggesting the absence of injury due to the procedure. An exception was observed for one animal that showed a continuous increase in the wall thickness. These effects may be explained by the large stent diameter and the placement site, close to the aortic bifurcation. Notably, the variations observed in the right artery and the aorta might be dependent on the size and location of the stents that varied between animals.

Moreover, we provide evidence that the wall thickness and the vessel diameter significantly correlated with the histological evaluation. Besides, histology provides evidence that the wall thickening in the stented area resulted in intimal hyperplasia. Neointimal hyperplasia was also observed in the left and right proximal control segments of two animals. Our results corroborate the well-established proliferation of smooth muscle cells resulting in the wall artery thickening induced by the stent and balloon injury [14–16].

In agreement with the literature, under conventional diet and following injury, rabbits developed wall hyperplasia that is known to be associated with inflammation and smooth muscle proliferation rather than atherosclerotic plaques that can be observed in hyperlipidemic rabbits [9, 17].

Although histological analysis is essential to evaluate wall composition, inflammation and smooth muscle proliferation, longitudinal study provides a useful tool to record transient variation in the vessel dimensions.

5. Conclusion

The non-invasive, real-time imaging of the rabbit iliac arteries and the distal abdominal aorta for the quantification of lumen diameter and wall thickness using high-resolution ultrasound permit the monitoring of the progression of the wall and vessel following balloon angioplasty and endovascular stent implantation. Conveniently combined with the blood flow analysis, this methodological approach would be essential to evaluate novel therapeutic approaches to prevent hyperplasia.

Acknowledgements

The study was supported by the Swiss National Science Foundation (SNF 316030_157658), the University of Fribourg and the Fonds Scientifique Cardiovasculaire FSC, Fribourg Hospital.

IntechOpen

Author details

Aurélien Frobert, Guillaume Ajalbert, Jérémy Valentin, Stéphane Cook and Marie-Noëlle Giraud*
Faculty of Sciences and Medicine, Cardiology, EMC Department, University of Fribourg, Switzerland

*Address all correspondence to: marie-noelle.giraud@unifr.ch

IntechOpen

References

[1] Benjamin EJ, Muntner P, Alonso A, Bittencourt MS, Callaway CW, Carson AP, et al. Heart disease and stroke statistics-2019 update: A report from the American Heart Association. Circulation. 2019;**139**(10):e56-e528

[2] Secemsky EA, Matteau A, Yeh RW, Steg PG, Camenzind E, Wijns W, et al. Comparison of short- and long-term cardiac mortality in early versus late stent thrombosis (from pooled PROTECT trials). The American Journal of Cardiology. 2015;**115**(12):1678-1684

[3] Conway C, Desany GJ, Bailey LR, Keating JH, Baker BL, Edelman ER. Fracture in drug-eluting stents increases focal intimal hyperplasia in the atherosclerosed rabbit iliac artery. Catheterization and Cardiovascular Interventions. 2019;**93**(2):278-285

[4] Tolva V, Mazzola S, Zerbi P, Casana R, Albertini M, Calvillo L, et al. A successful experimental model for intimal hyperplasia prevention using a resveratrol-delivering balloon. Journal of Vascular Surgery. 2016;**63**(3):788-794

[5] Nishio H, Masumoto H, Sakamoto K, Yamazaki K, Ikeda T, Minatoya K. MicroRNA-145-loaded poly(lactic-co-glycolic acid) nanoparticles attenuate venous intimal hyperplasia in a rabbit model. The Journal of Thoracic and Cardiovascular Surgery. 2019;**157**(6):2242-2251

[6] Jain M, Zellweger M, Wagnieres G, van den Bergh H, Cook S, Giraud MN. Photodynamic therapy for the treatment of atherosclerotic plaque: Lost in translation? Cardiovascular Therapeutics. 2017;**35**(2):e12238

[7] Lanvin T, Conkey DB, Frobert A, Valentin J, Goy JJ, Cook S, et al. Subsurface ablation of atherosclerotic plaque using ultrafast laser pulses. Biomedical Optics Express. 2015;**6**(7):2552-2561

[8] Lin W, Qin L, Qi H, Zhang D, Zhang G, Gao R, et al. Long-term in vivo corrosion behavior, biocompatibility and bioresorption mechanism of a bioresorbable nitrided iron scaffold. Acta Biomaterialia. 2017;**54**:454-468

[9] Zaragoza C, Gomez-Guerrero C, Martin-Ventura JL, Blanco-Colio L, Lavin B, Mallavia B, et al. Animal models of cardiovascular diseases. Journal of Biomedicine and Biotechnology. 2011;**2011**:497841

[10] Jain M, Frobert A, Valentin J, Cook S, Giraud MN. The rabbit model of accelerated atherosclerosis: A methodological perspective of the iliac artery balloon injury. Journal of Visualized Experiments. 2017;(128)

[11] Newby AC. An overview of the vascular response to injury: A tribute to the late Russell Ross. Toxicology Letters. 2000;**112-113**:519-529

[12] Welt FG, Tso C, Edelman ER, Kjelsberg MA, Paolini JF, Seifert P, et al. Leukocyte recruitment and expression of chemokines following different forms of vascular injury. Vascular Medicine. 2003;**8**(1):1-7

[13] Virmani R, Kolodgie FD, Farb A, Lafont A. Drug eluting stents: Are human and animal studies comparable? Heart. 2003;**89**(2):133-138

[14] Chaabane C, Otsuka F, Virmani R, Bochaton-Piallat ML. Biological responses in stented arteries. Cardiovascular Research. 2013;**99**(2):353-363

[15] Carter AJ, Laird JR, Farb A, Kufs W, Wortham DC, Virmani R. Morphologic characteristics of lesion formation

and time course of smooth muscle cell proliferation in a porcine proliferative restenosis model. Journal of the American College of Cardiology. 1994;**24**(5):1398-1405

[16] Curcio A, Torella D, Indolfi C. Mechanisms of smooth muscle cell proliferation and endothelial regeneration after vascular injury and stenting: Approach to therapy. Circulation Journal. 2011;**75**(6):1287-1296

[17] Yamashita A, Asada Y. A rabbit model of thrombosis on atherosclerotic lesions. Journal of Biomedicine and Biotechnology. 2011;**2011**:424929